Relativistic random-phase approximation calculation with negative energy states of nuclear polarization in muonic atoms

Akihiro Haga,[1,*] Yataro Horikawa,[2,†] Yasutoshi Tanaka,[3,‡] and Hiroshi Toki[1,§]
[1]*Research Center for Nuclear Physics (RCNP), Osaka University, Ibaraki, Osaka 567-0047, Japan*
[2]*Department of Physics, Juntendo University, Inba-gun, Chiba 270-1695, Japan*
[3]*Department of Environmental Technology and Urban Planning, Nagoya Institute of Technology, Gokiso, Nagoya 466-8555, Japan*
(Received 14 January 2004; published 15 April 2004)

We study the muonic nuclear-polarization corrections, which provide level shifts due to the two-photon exchange process between a bound muon and a nucleus. We choose ^{16}O as a nucleus for the demonstration of the amount and the property of the nuclear polarization in the muonic atoms. The nuclear states of ^{16}O are constructed in the random-phase approximation including the negative-energy states based on the relativistic mean field model. The spatial components of the transition current have large couplings between positive- and negative-energy states. As a result, the contribution from the negative-energy states of nucleus to the nuclear-polarization correction is found to be significant and also essential to achieve gauge invariance. The nuclear-polarization effect in muonic ^{16}O is also calculated using the collective model. We find that the nonrelativistic nuclear model with the effective mass provides similar results as the relativistic one.

DOI: 10.1103/PhysRevC.69.044308 PACS number(s): 36.10.Dr, 12.20.Ds, 21.60.Jz, 31.30.Jv

I. INTRODUCTION

High-precision measurements of the energy levels in muonic atoms and highly charged ions recently available in the relativistic heavy ion collisions have provided a sensitive test of quantum electrodynamics (QED) in strong external electromagnetic fields. (See Refs. [1,2] and references therein.) In the evaluation of the energy levels of muonic or heavy hydrogenlike atoms precisely, it is also required to take into account the effects that electromagnetic fields of the muon or the electron polarize the nucleus. The level shift due to these effects is traditionally called "nuclear polarization" (NP), and the study of the NP contribution to the energy shift of atomic levels is important as a background effect against the QED corrections in ordinary atoms, while it is one of the main corrections in muonic atoms.

The calculations of the NP correction, which take into account the retarded transverse part as well as the longitudinal part of photon propagator, were recently presented in electronic and muonic ^{208}Pb with the nonrelativistic random-phase approximation (RPA) [3,4]. The NP corrections in ^{208}Pb and ^{238}U were also calculated with the nuclear collective model [5]. In these studies, the ladder, cross, and seagull diagrams in the two-photon exchange process were considered as the lowest-order NP correction. The common features of the results of these analyses show that, without the inclusion of the seagull diagrams, there exists a large violation of the gauge invariance in the NP results.

The seagull diagram comes from the minimal prescription of the electromagnetic coupling for the nonrelativistic Hamiltonian of nucleon [6,7], in which the antinucleon degree of freedom is eliminated. The NP calculation in the relativistic field theoretical nuclear model, therefore, is interesting in the viewpoint that the negative-energy states of nucleus contribute instead of the seagull diagram. The fact that the seagull diagram has a significant role to obtain the gauge-invariant NP correction suggests that the effect of the negative-energy states plays an important role in the NP calculation in a relativistic model of nuclei.

Phenomenological relativistic field theories based on hadrons, referred to as quantum hadrodynamics (QHD) [8], have been successful in describing the bulk and single-particle properties of nuclei in the mean field approximation. When the energy functional of the mean field theory (MFT) is fitted to nuclear saturation, they automatically produce an appropriate order of the spin-orbit splitting of nuclei, the spin observables of the proton-nucleus scattering, and energy dependence of the proton-nucleus optical potential. Nuclear excitations also have been investigated by QHD using the relativistic random-phase approximation (RRPA) with the MFT basis [9–12]. In the previous calculations in Refs. [9,13,14], where the spectral method is used to solve the RRPA equation, the configuration space is restricted to ordinary particle-hole pairs. This seems a reasonable approximation at first sight, since the excitation of the negative-energy states in the Dirac sea to the positive-energy states has an unperturbed energy more than 1.2 GeV. Due to the huge binding of the negative-energy states in the QHD model, however, it was found that the negative-energy states are needed in RRPA to preserve current conservation for the transition currents, to decouple the spurious translational states, and to reproduce the excitation energies and transition form factors obtained by the nonspectral RRPA in which the negative-energy contribution is included automatically [15–18].

In the present paper, we take the RRPA + MFT method of QHD to generate the nuclear intermediate states for the NP calculation. The essential features of the phenomenological

*Electronic address: haga@rcnp.osaka-u.ac.jp
†Electronic address: horikawa@sakura.juntendo.ac.jp
‡Electronic address: tanakay@nitech.ac.jp
§Electronic address: toki@rcnp.osaka-u.ac.jp

QHD model are that nucleon scalar and vector self-energies are very large, and cancel each other to provide the usual binding energy in the nucleon sector. This means that there is a very strong attractive self-energy in the antinucleon sector leading to large binding of antinucleon. Since the negative-energy contribution is expected to play essential role in the NP calculation, the NP calculation with QHD may confirm or rule out this very large binding through its sensitivity to the contribution from the negative-energy states.

For this purpose, the NP calculation for heavy muonic atoms and heavy hydrogenlike ions is certainly more suitable because the antinucleon effects are expected to be large [3,4]. Unfortunately, the necessity of negative-energy states in the relativistic calculation means that the RRPA equation must be solved under the huge configuration space for heavy nuclei. Therefore, for the purpose of demonstrating the antinucleon effect to the NP correction, we calculate the NP correction for $1s_{1/2}$ state in muonic ^{16}O for which the configuration space is not so large, while enough number of negative-energy states are obtained. A large overlap of the muon wave function with the nucleus enables us to perform precise numerical calculations in comparison with the electronic NP calculations.

This paper is organized as follows. In Sec. II A, we first give general formulas needed for the evaluation of the NP correction and then explain the present RRPA calculation in Sec. II B. In Sec. II C, the effective single-particle operator used in the calculation of the transition form factors is explained with respect to the charge conservation and gauge invariance. The details of the present spectral RRPA + MFT calculation is explained and numerical accuracy of the NP results is discussed in Sec. II D. In Sec. III, we present the result of the NP correction in muonic ^{16}O and discuss the role of gauge invariance, the reason of large contribution from the antinucleon states, and the difference from nonrelativistic calculation. In Sec. IV, we give summary of the present analysis.

II. RELATIVISTIC NUCLEAR-POLARIZATION CORRECTION

A. Formalism for nuclear-polarization correction

The interaction between the muon and the nucleus is described by the interaction-Hamiltonian density

$$\hat{\mathcal{H}}_I = e\hat{j}_M^\mu \hat{A}_\mu + e\hat{j}_N^\mu \hat{A}_\mu, \tag{1}$$

where $\hat{j}_M^\mu$ ($\hat{j}_N^\mu$) is the muonic (nuclear) current operator and $\hat{A}_\mu$ is the electromagnetic field operator. Following the S-matrix theory [19,20], the lowest-order NP correction for the interaction-Hamiltonian density of Eq. (1) in the natural unit with $\hbar = c = 1$ and $e^2 = 4\pi\alpha$ is given by [21]

$$\Delta E_{NP} = i(4\pi\alpha)^2 \int d^4x_1 \cdots d^4x_4 \overline{\psi}_M(x_1)\gamma^\mu S_F^M(x_1,x_2)\gamma^\nu \psi_M(x_2) \times D_{\mu\xi}(x_1,x_3)\Pi_N^{\xi\zeta}(x_3,x_4)D_{\zeta\nu}(x_4,x_2). \tag{2}$$

Here ψ_M is the muon wave function, S_F^M is the external-field muon propagator, $D_{\mu\xi}$ is the photon propagator, and $\Pi_N^{\xi\zeta}$ is the nuclear-polarization tensor which contains all information of nuclear dynamics. Using the spectral representation of the Feynman propagator, the muonic parts of Eq. (2) is written as

$$\overline{\psi}_M(x_1)\gamma^\mu S_F^M(x_1,x_2)\gamma^\nu \psi_M(x_2) = \int \frac{dE}{2\pi} e^{-iE(t_1-t_2)} \sum_{i'} \frac{j_M^\mu(\boldsymbol{x}_1)_{ii'} j_M^\nu(\boldsymbol{x}_2)_{i'i}}{E - \omega_M + iE_{i'}\epsilon}, \tag{3}$$

where $\omega_M = E_{i'} - E_i$ is the excitation energy of the muon, and

$$j_M^\mu(\boldsymbol{x})_{ii'} = \overline{\psi}_{M_i}(\boldsymbol{x})\gamma^\mu \psi_{M_{i'}}(\boldsymbol{x}) \tag{4}$$

is the transition current density of the muon. The suffixes i and i' stand for the initial and intermediate states of the muon, respectively.

The nuclear-polarization part $\Pi_N^{\xi\zeta}(x_3,x_4)$ in RRPA is written as

$$\Pi_N^{\xi\zeta}(x_3,x_4) = \int \frac{d\omega}{2\pi} e^{-i\omega(t_3-t_4)} \sum_{I'} \left(\frac{J_N^\xi(\boldsymbol{x}_3)_{II'} J_N^\zeta(\boldsymbol{x}_4)_{I'I}}{\omega - \omega_N + iE_{I'}\epsilon} - \frac{J_N^\zeta(\boldsymbol{x}_4)_{II'} J_N^\xi(\boldsymbol{x}_3)_{I'I}}{\omega + \omega_N - iE_{I'}\epsilon} \right), \tag{5}$$

where $J_N^\xi(\boldsymbol{x})_{II'}$ is the transition current density calculated with the RRPA and $\omega_N = E_{I'} - E_I$ is excitation energy of the nucleus. The suffixes I and I' stand for the initial and intermediate states of the nucleus, respectively. It should be noted that, in Eq. (5), the positions of poles depend on the sign of the excitation energy since the excited states I' include the negative-energy eigenstates which correspond to Pauli blocking of the vacuum polarization.

After substituting Eqs. (3) and (5) into Eq. (2), and performing the integral over all time variables, we transfer the expressions for the nuclear-polarization energies to the momentum space. For the NP energy shifts due to the ladder and cross diagrams depicted in Fig. 1, we obtain

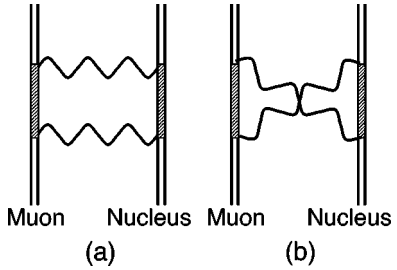

FIG. 1. Diagrams contributing to the nuclear polarization in the lowest order: (a) ladder and (b) cross diagrams. The wavy line denotes photon, while the double straight lines denote the muon and the nucleus.

$$\Delta E^L_{NP} = -i(4\pi\alpha)^2 \int \frac{d\omega}{2\pi} \int \frac{d\boldsymbol{q}}{(2\pi)^3} \int \frac{d\boldsymbol{q}'}{(2\pi)^3} D_{\mu\xi}(\omega,\boldsymbol{q}) D_{\zeta\nu}(\omega,\boldsymbol{q}') \times \sum_{i'} \frac{j^\mu_e(-\boldsymbol{q})_{ii'} j^\nu_e(\boldsymbol{q}')_{i'i}}{\omega + \omega_e - iE_{i'}\epsilon} \sum_{I'} \frac{J^\xi_N(\boldsymbol{q})_{II'} J^\zeta_N(-\boldsymbol{q}')_{I'I}}{\omega - \omega_N + iE_{I'}\epsilon} \tag{6}$$

and

$$\Delta E^X_{NP} = i(4\pi\alpha)^2 \int \frac{d\omega}{2\pi} \int \frac{d\boldsymbol{q}}{(2\pi)^3} \int \frac{d\boldsymbol{q}'}{(2\pi)^3} D_{\mu\xi}(\omega,\boldsymbol{q}) D_{\zeta\nu}(\omega,\boldsymbol{q}') \times \sum_{i'} \frac{j^\mu_e(-\boldsymbol{q})_{ii'} j^\nu_e(\boldsymbol{q}')_{i'i}}{\omega + \omega_e - iE_{i'}\epsilon} \sum_{I'} \frac{J^\zeta_N(-\boldsymbol{q}')_{II'} J^\xi_N(\boldsymbol{q})_{I'I}}{\omega + \omega_N - iE_{I'}\epsilon}, \tag{7}$$

respectively. The total NP correction is given by the sum $\Delta E^L_{NP} + \Delta E^X_{NP}$.

We evaluate the NP correction both in the Feynman and Coulomb gauges for the photon propagator. In Eqs. (6) and (7), ω integrations can be carried out analytically for photon propagators in both gauges, taking the singularities of Eqs. (3) and (5) into account properly in the contour integration. After the integration over ω, the formulas for the Feynman and Coulomb gauges can be obtained as explained in Ref. [3]. Then, angular integral over $\boldsymbol{q}$ and $\boldsymbol{q}'$ in Eqs. (6) and (7) can be carried out after multipole expansion of the muonic and nuclear form factors. Hence, only q and q' remain to be integrated numerically. The nuclear-polarization correction is thus given by the sum of these double integrals over the nuclear and muon intermediate states.

B. Relativistic random-phase approximation

In QHD, the nucleus is described as a system of Dirac nucleons which interact in a relativistic covariant manner through the exchange of virtual mesons and photons [8]. We employ the following Lagrangian density in the present calculation:

$$\begin{aligned}\mathcal{L}_N = {} & \bar{\psi}_N (i\gamma^\mu \partial_\mu - m_N)\psi_N + \frac{1}{2}(\partial_\mu \sigma \partial^\mu \sigma - m_\sigma^2 \sigma^2) - \frac{1}{3} g_2 \sigma^3 - \frac{1}{4} g_3 \sigma^4 - \frac{1}{4}(\partial_\mu \omega_\nu - \partial_\nu \omega_\mu)^2 + \frac{1}{2} m_\omega^2 \omega_\mu \omega^\mu \\ & - \frac{1}{4}(\partial_\mu \boldsymbol{\varrho}_\nu - \partial_\nu \boldsymbol{\varrho}_\mu)^2 + \frac{1}{2} m_\varrho^2 \boldsymbol{\varrho}_\mu \cdot \boldsymbol{\varrho}^\mu - \frac{1}{4}(\partial_\mu A_\nu - \partial_\nu A_\mu)^2 - g_\sigma \bar{\psi}_N \sigma \psi_N - g_\omega \bar{\psi}_N \gamma_\mu \omega^\mu \psi_N \\ & - \frac{1}{2} g_\varrho \bar{\psi}_N \gamma_\mu \boldsymbol{\varrho}^\mu \cdot \boldsymbol{\tau} \psi_N - e \bar{\psi}_N \gamma_\mu A^\mu \mathcal{Q} \psi_N + \frac{e\kappa_N}{4m_N} \bar{\psi}_N \sigma^{\mu\nu}(\partial_\mu A_\nu - \partial_\nu A_\mu)\psi_N. \end{aligned} \tag{8}$$

This Lagrangian density is based on the nonlinear σ-ω model with $\boldsymbol{\varrho}$ meson and the photon field A added. While $\boldsymbol{\varrho}$ meson is required to describe the isospin $T=1$ states, there is no contribution from $\boldsymbol{\varrho}$ meson in the MFT calculation of ^{16}O. In Eq. (8), $\mathcal{Q}=(1+\tau_3)/2$ projects proton and $\kappa_p = 1.7928$ and $\kappa_n = -1.9131$. Assuming that the nuclear ground state is spherically symmetric, the MFT basis is constructed from eigenfunctions of the following Dirac equation:

$$[\gamma^0(\varepsilon_\alpha - g_\omega \omega_0 - \tfrac{1}{2} g_\varrho \tau^3 \varrho_0^3 - \mathcal{Q}A_0) + i\boldsymbol{\gamma}\cdot\boldsymbol{\nabla} - (m_N + g_\sigma \sigma)]\psi_{N\alpha} = 0, \tag{9}$$

in which there are solutions for the negative energies in Dirac sea as well as the ordinary positive energies. The continuum states are discretized by "putting the system in a box" and thus we express the MFT Green function in terms of the basis $\psi_{N\alpha}$ via a spectral expansion.

The RRPA polarization insertion is represented by polarization insertion constructed from the MFT Green function and two-body interaction between the nucleons. Following the RRPA prescription for discrete states described in Ref. [15], RRPA matrix equation is given as

$$\sum_{\lambda\mu} \begin{pmatrix} A_{\alpha\beta:\lambda\mu} & B_{\alpha\beta:\lambda\mu} \\ -B_{\alpha\beta:\lambda\mu} & -A_{\alpha\beta:\lambda\mu} \end{pmatrix} \begin{pmatrix} X^{(N)}_{\lambda\mu} \\ Y^{(N)}_{\lambda\mu} \end{pmatrix} = \omega_N \begin{pmatrix} X^{(N)}_{\alpha\beta} \\ Y^{(N)}_{\alpha\beta} \end{pmatrix}, \tag{10}$$

where,

$$A_{\alpha\beta:\lambda\mu} = [\delta_{\beta\mu}\delta_{\alpha\lambda}\omega_{\alpha\beta} + V_{\alpha\beta:\lambda\mu}(\omega_N)], \tag{11}$$

$$B_{\alpha\beta:\lambda\mu} = V_{\alpha\beta:\mu\lambda}(\omega_N). \tag{12}$$

The indices α and λ label the particle space, while the indices β and μ label the hole space. Here, the hole labels β and μ are restricted to positive-energy occupied levels. On the other hand, the particle labels α and λ indicate entire MFT spectrum, including the negative-energy levels which take care of the Pauli blocking of the response of vacuum. The forward and backward amplitudes of particle-hole pairs are denoted by X and Y, respectively. In the RRPA kernel, $\omega_{\alpha\beta}$ is the difference between ε_α and ε_β which are the eigenvalues of the Dirac equation (9), and

TABLE I. Parameter sets used in the present calculations.

	m_N	m_σ	m_ω	m_ρ	g_σ	g_2	g_3	g_ω	g_ρ
HS	939.0	520.0	783.0	770.0	10.47	0.0	0.0	13.80	8.08
NL-SH	939.0	526.06	783.0	763.0	10.44	−6.91	−15.83	12.95	8.77

$$V_{\alpha\beta:\lambda\mu}(\omega_N) = \int d\boldsymbol{r}d\boldsymbol{r}'[\bar{\psi}_{N\alpha}(\boldsymbol{r})\bar{\psi}_{N\mu}(\boldsymbol{r}')V(\boldsymbol{r}-\boldsymbol{r}')\psi_{N\beta}(\boldsymbol{r})\psi_{N\lambda}(\boldsymbol{r}')], \tag{13}$$

where

$$V(\boldsymbol{r}-\boldsymbol{r}') = -\frac{g_\sigma^2}{4\pi}D^\sigma(\boldsymbol{r}-\boldsymbol{r}';\omega_N) + \frac{g_\omega^2}{4\pi}D^\omega_{\mu\nu}(\boldsymbol{r}-\boldsymbol{r}';\omega_N)(\gamma^\mu)(\gamma^\nu) + \frac{g_\varrho^2}{4\pi}D^\varrho_{\mu\nu}(\boldsymbol{r}-\boldsymbol{r}';\omega_N)(\gamma^\mu\boldsymbol{\tau})\cdot(\gamma^\nu\boldsymbol{\tau}) + \frac{e^2}{4\pi}D^A_{\mu\nu}(\boldsymbol{r}-\boldsymbol{r}';\omega_N)(\gamma^\mu\mathcal{Q})(\gamma^\nu\mathcal{Q}) \tag{14}$$

is used as a two-body interaction. Here, D^σ, $D^\omega_{\mu\nu}$, $D^\varrho_{\mu\nu}$, and $D^A_{\mu\nu}$ denote σ, ω, ϱ mesons, and photon propagators, respectively. The propagator of σ meson is modified from Yukawa form due to the nonlinear term. In this calculation, we employ the uncharged ϱ-meson interaction in order to describe the isospin $T=1$ states. For simplicity, residual mesons, i.e., pion, charged ϱ meson, and so on, are not considered.

In these equations, ω_N is the energy difference between the RRPA excited state and the ground state. The dependence of ω_N may be usually ignored in the calculation for the low-lying states with the excitation energy much smaller than the meson masses [16]. The RRPA negative-energy states that we take into account, however, involve the states generated from the Dirac sea, hence the excitation energies are larger than the meson masses. Therefore, it may not be justified to set $\omega_N=0$ neglecting the retardation. However, if we retain the retardation in the RRPA interaction in Eqs. (11) and (12), the proof of the current conservation and the gauge invariance no longer hold because the nuclear intermediate states do not have a completeness relation any longer [3]. Then, the NP corrections calculated by RRPA *do not satisfy* gauge invariance. In the present calculation, we regard the effect of the retardation as a higher-order correction studied in a future work and ignore it. The parameter sets we have chosen in the present calculation are given in Table I. The linear version of the relativistic mean field Lagrangian called HS [22] is used while the nonlinear version called NL-SH [23] is used out of various nonlinear versions as NL3 [24] and TM1 [25].

C. Transition current densities

To calculate the transition current densities of the nucleus, the following electromagnetic current operators are usually used with the relativistic Hartree wave functions:

$$\hat{j}^\mu_N = \hat{\bar{\psi}}_N\gamma^\mu\mathcal{Q}\hat{\psi}_N + \frac{\kappa_N}{2m_N}\partial_\nu(\hat{\bar{\psi}}_N\sigma^{\mu\nu}\hat{\psi}_N), \tag{15}$$

where the second term is the anomalous current operator. The charge and three-vector current operators, $\hat{\varrho}_N$ and $\hat{\boldsymbol{j}}_N$, are given by

$$\hat{\varrho}_N = \hat{\psi}^\dagger\mathcal{Q}\hat{\psi} + \frac{i\kappa_N}{2m_N}\boldsymbol{\nabla}\cdot\hat{\psi}^\dagger\beta\boldsymbol{\alpha}\hat{\psi}, \tag{16}$$

$$\hat{\boldsymbol{j}}_N = \hat{\psi}^\dagger\boldsymbol{\alpha}\mathcal{Q}\hat{\psi} + \frac{\kappa_N}{2m_N}\boldsymbol{\nabla}\times\left[\hat{\psi}^\dagger\begin{pmatrix}\boldsymbol{\sigma} & 0\\ 0 & -\boldsymbol{\sigma}\end{pmatrix}\hat{\psi}\right] - \frac{\kappa_N}{2m_N}\frac{\partial}{\partial t}\hat{\psi}^\dagger\gamma\hat{\psi}, \tag{17}$$

respectively.

To obtain the gauge-invariant result in the two-photon exchange process without the seagull contribution, it is required that the commutation relation between the charge and current operators vanishes. However, it is easy to see that the charge-current operators of Eqs. (16) and (17) *do not commute*. We shall eliminate the second term in Eq. (16) and the third term in Eq. (17), which cause the noncommutation between charge and current operators. (More detailed argument for this prescription is given in the Appendix.) Thus, we use the following operators in the calculation of the NP correction:

$$\hat{\varrho}_N = \hat{\psi}^\dagger\hat{\mathcal{Q}}\hat{\psi}, \tag{18}$$

$$\hat{\boldsymbol{j}}_N = \hat{\psi}^\dagger\boldsymbol{\alpha}\hat{\mathcal{Q}}\hat{\psi} + \frac{\kappa_N}{2m_N}\boldsymbol{\nabla}\times\left[\hat{\psi}^\dagger\begin{pmatrix}\boldsymbol{\sigma} & 0\\ 0 & -\boldsymbol{\sigma}\end{pmatrix}\hat{\psi}\right]. \tag{19}$$

The multipole form factors are defined by the Fourier transform of transition current densities as

$$\langle I'\|M_\lambda(q)\|I\rangle = \int d\boldsymbol{x}j_\lambda(qx)\langle I'\|Y_\lambda(\Omega_x)\varrho_N(\boldsymbol{x})\|I\rangle, \tag{20}$$

$$\langle I'\|T_{\lambda L}(q)\|I\rangle = \int d\boldsymbol{x} j_L(qx)\langle I'\|\boldsymbol{Y}_{\lambda L}(\Omega_x)\cdot\boldsymbol{j}_N(\boldsymbol{x})\|I\rangle, \quad (21)$$

where $j_\lambda(qx)$ is a spherical Bessel function. $\boldsymbol{Y}_{\lambda L}$ is a vector spherical harmonics and λ is the multipolarity of transition. If RRPA equation is solved without truncation of basis, it is known that transition charge and current densities satisfy the charge conservation relation [15,16]

$$\langle I'\|M_\lambda(q)\|I\rangle = -\frac{q}{\omega_N}\sqrt{\frac{\lambda}{2\lambda+1}}\langle I'\|T_{\lambda\lambda-1}(q)\|I\rangle + \frac{q}{\omega_N}\sqrt{\frac{\lambda+1}{2\lambda+1}}\langle I'\|T_{\lambda\lambda+1}(q)\|I\rangle. \quad (22)$$

As shown in the following section, the electromagnetic RRPA transition current is sufficiently conserved with the present calculation.

D. Numerical detail

We shall explain here the main aspects of solving the RRPA equation. The RRPA equation can be solved using either "spectral" or "nonspectral" methods. The completeness of the basis is conveniently treated by the nonspectral method where negative-energy contribution is included automatically [15,16]. However, NP calculation involves the integral over the loop variables ω, and this can be performed analytically only in the spectral method. Thus there is some trade-off between the integration over the nuclear intermediate states and the loop integrations. Moreover, we are not certain whether the singularity structure in the complex energy plane which is crucial in the loop integral is properly treated by the nonspectral method used in the above references.

Therefore we have employed the spectral method to solve the RRPA equation. First, Eq. (10) is written for each angular momentum and isospin. In the nonrelativistic case, then, it can be reduced to a Hermitian eigenvalue problem of half dimension [26]. In the relativistic case, however, the RRPA equation can no longer be reduced to a Hermitian problem of half dimension, because the sum or difference of partial matrices of Eq. (10), $(A\pm B)$, is not positive definite due to the negative-energy state in the MFT basis. As a result, we have to solve the RRPA eigenvalues and eigenvectors by computing the left and right eigenvectors of $(A+B)(A-B)$.

In heavy nuclei, the necessity of negative-energy states means that the RRPA equation must be solved under the huge configuration space. Therefore, for the purpose of seeing the effect of antinucleon states to the NP correction, we choose ^{16}O for which configuration space is not so large, while enough number of antinucleon states are obtained. We calculate the NP correction for $1s_{1/2}$ muon state since the NP effect for electronic O^{16} is much smaller.

The MFT basis functions in the RRPA calculation are obtained by solving the single-particle Dirac equation (9), using the method of discretization for the continuum states, as shown in Ref. [16]. For the calculation of excitation states of ^{16}O used in the NP calculation, we have included the positive-energy states up to 250 MeV and practically all of the negative-energy bound states. There are a large number of bound states in the negative-energy spectrum because the scalar and vector potentials add in the effective negative-energy potential.

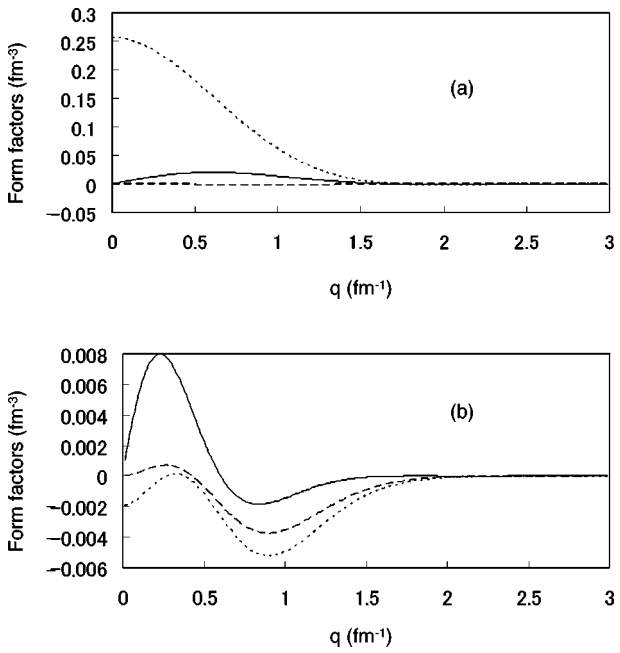

FIG. 2. Nuclear form factors for the isoscalar 1^- state obtained in the RRPA calculation with HS: (a) the 1076 MeV highest negative-energy state and (b) the 8.5 MeV lowest positive-energy state in ^{16}O. The longitudinal and transverse form factors $\langle I'\|M_1(q)\|I\rangle$, $\langle I'\|T_{10}(q)\|I\rangle$, and $\langle I'\|T_{12}(q)\|I\rangle$ are displayed by the solid, dotted, and dashed curves, respectively.

The resulting RRPA equation has the eigenstates with the negative energy, which we shall hereafter refer to as the antinucleon states in order to distinguish them from the negative-energy states of the MFT basis. The contribution from these states represents the blocking effect of the nucleon-antinucleon creation due to the states occupied by the spectator nucleon. The longitudinal and transverse form factors for the 1^- state with the transition energy of −1076 MeVare shown in Fig. 2(a). The transverse form factor is an order of magnitude larger than that of the positive-energy 1^- state shown in Fig. 2(b). It is also seen that the form factors of antinucleon states have a peak in a very lower momentum than the corresponding transition energy, because the states are bound strongly. Thus, the form factors of the vacuum polarized states overlap with the muonic form factors and give the non-negligible contribution in the NP correction.

The violation of charge-current conservation in the transition densities, defined by the difference between the left-hand and right-hand sides of Eq. (22) (hereafter referred to as $\Delta\varrho$), is very small with a large configuration space showing that our truncation is reasonable. Figure 3 shows the $\Delta\varrho$ for the lowest positive-energy 1^- state with each configuration space truncated by energies of 40, 80, 150, and 250 MeV, and the 250 MeV without the negative-energy states. It is found that the charge-current conservation is satisfied very well in the calculation truncated by energy of 250 MeV with

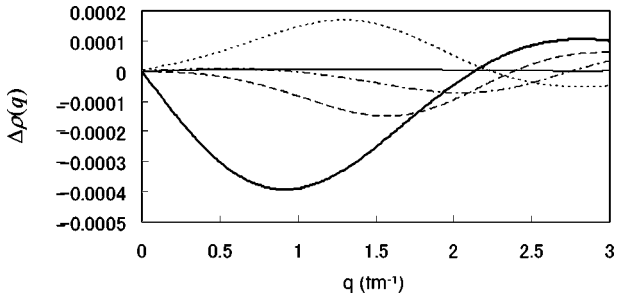

FIG. 3. Violation of charge-current conservation in the transition densities $\Delta\varrho$ for the lowest positive-energy isoscalar 1^- state in ^{16}O. The results of the calculation with configuration space truncated by the energies of 40, 80, 150, 250 MeV, and 250 MeV without the negative-energy states are displayed by the dotted, dashed, dash-dotted, solid, and thick-solid curves, respectively. The parameter set HS is employed.

negative-energy states included, and confirmed the importance of the negative-energy states for a correct description of the transition currents as pointed out in Ref. [16].

In electronic atoms with the much larger size of the electronic orbits, it is well known that the NP energy shifts induced by the Coulomb interaction are approximately in proportion to the reduced electric transition probabilities [21]. Hence, it is useful for the discussion of the muonic NP correction in light nuclei to present the energy-weighted sum of the reduced matrix element $B(E\lambda)$ calculated by the relativistic nuclear model. The result for ^{16}O is shown in Table II, where we take the summation over only the positive-energy states in the RRPA excitation. Both in HS and NL-SH, the present results are somewhat larger than the classical energy-weighted sum rule (EWSR) values of Ref. [27] in any multipole states. The reason has been presumed as due to the effective mass m_N^* in Ref. [15]. Certainly, our EWSR agrees better with the classical EWSR value when the effective mass is used as shown in the fourth column of Table II. In addition, this role of the effective mass explains the result that EWSR values in HS become larger than those in NL-SH; HS provides smaller effective mass as compared to NL-SH in the nuclear matter calculation.

In passing, we mention that since the charge operator of Eq. (18) commutes with the single-particle Hamiltonian of nucleus, the EWSR value vanishes in the present calculation if the vacuum polarized states with negative energies are also taken into account in the sum. The result is that the RRPA states satisfy a completeness relation by including the antinucleon states.

III. RESULTS AND DISCUSSION

We calculate the nuclear-polarization correction here by computing an energy shift due to each multipole of the excitations and summing the results. The 0^+, 1^-, and 2^+ nuclear states up to 250 MeV excitations in the positive-energy states and −1870 MeV in the antinucleon states are taken into account in the present calculation. The muonic $1s_{1/2}$ state has been calculated by solving the Dirac equation with the finite Coulomb potential due to the charge distribution of ^{16}O [3].

Tables III and IV summarize the NP correction of the $1s_{1/2}$ state for muonic ^{16}O by parameter sets HS and NL-SH, respectively. In these tables, the first column denotes nuclear spin parities. The + and − in the second column indicate the contributions from the positive-energy states and the antinucleon states of ^{16}O to the NP correction, while the + and − in the third column indicate the contributions from the positive- and negative-energy states of the muon to the NP correction. The fourth column shows the results in the Feynman gauge, while the fifth column shows the results in the Coulomb gauge. Finally, the last column shows the Coulomb NP correction, which is the result in the Coulomb gauge without the transverse-photon contribution.

From Tables III and IV, we see that the linear and the nonlinear models give the similar result in the NP correction. The slight difference between them comes from the effective mass as mentioned for the EWSR in the preceding section. For both the parameter sets, the NP corrections in the Feynman and Coulomb gauges agree fairly well. The results are gauge invariant for each multipole excitation. This means that the completeness for the intermediate states of the muon and ^{16}O nucleus is quite satisfactory by present truncation of the configuration space.

It is also found that the antinucleon states contributions are about 8% in the Feynman gauge and 4% in Coulomb gauge of the total NP correction in spite of its large excitation energy more than 1 GeV. An interesting feature of the results is that a violation of gauge invariance occurs due to the different contributions of antinucleon states between gauges, if the antinucleon states are not taken into account;

TABLE II. Energy-weighted sums of $B(E\lambda)$ over positive-energy RRPA states in unit of $e^2\, b^\lambda$ MeV. The classical EWSR values [27] with and without effective mass are also shown for comparison. The effective mass m_N^* is calculated by MFT with the HS parameter set.

$E\lambda$	Present (HS)	Present (NL-SH)	Classical (m_N)[a]	Classical (m_N^*)[a]
$E0$[b]	0.0416	0.0394	0.0350	0.0460
$E1$[c]	0.8052	0.7835	0.5940	0.8637
$E2$	0.5211	0.4940	0.4372	0.5745

[a]The radial moments $\langle r^\lambda\rangle_p$ in the classical EWSR are calculated with the charge distribution from the MFT with parameter set HS.
[b]The $E0$ operator is defined as $O(E0)=\Sigma_p r^2/\sqrt{4\pi}$.
[c]The $E1$ operator is defined as $O(E1)=\Sigma_i -1/2\,\tau_3 r Y_{1\mu}$.

TABLE III. Nuclear-polarization correction (eV) to the $1s_{1/2}$ state of muonic ^{16}O with the parameter set HS. In the column ω_N (ω_μ), + denotes contribution from ordinary positive-energy states of ^{16}O (muon), while − denotes contribution from antinucleon (antimuon) states.

λ^π	ω_N	ω_μ	Feynman[a]	Coulomb[b]	CNP[c]
0^+	+	+	−0.821	−0.822	−0.822
	+	−	+0.053	+0.039	+0.039
	−	+	+0.017	+0.001	+0.001
	−	−	−0.030	−0.000	−0.000
	Total		−0.781	−0.782	−0.782
1^-	+	+	−8.878	−8.917	−8.513
	+	−	+0.820	+0.518	+0.135
	−	+	+0.292	+0.167	+0.004
	−	−	−1.021	−0.556	−0.001
	Total		−8.787	−8.788	−8.375
2^+	+	+	−1.458	−1.462	−1.387
	+	−	+0.183	+0.152	+0.085
	−	+	+0.083	+0.047	+0.002
	−	−	−0.149	−0.081	−0.000
	Total		−1.341	−1.343	−1.301
Total	+	+	−11.157	−11.202	−10.723
	+	−	+1.056	+0.710	+0.259
	−	+	+0.392	+0.216	+0.007
	−	−	−1.200	−0.637	−0.001
	Total		−10.910	−10.913	−10.458

[a]The NP correction in the Feynman gauge.
[b]The NP correction in the Coulomb gauge.
[c]The NP correction in the Coulomb gauge without transverse part.

TABLE IV. Same as Table III, except for the parameter set NL-SH is employed in the NP calculation.

λ^π	ω_N	ω_μ	Feynman[a]	Coulomb[b]	CNP[c]
0^+	+	+	−0.723	−0.724	−0.724
	+	−	+0.051	+0.038	+0.038
	−	+	+0.017	+0.001	+0.001
	−	−	−0.030	−0.000	−0.000
	Total		−0.685	−0.685	−0.685
1^-	+	+	−8.149	−8.185	−7.789
	+	−	+0.779	+0.482	+0.131
	−	+	+0.286	+0.164	+0.004
	−	−	−0.990	−0.541	−0.000
	Total		−8.074	−8.076	−7.654
2^+	+	+	−1.350	−1.353	−1.289
	+	−	+0.171	+0.142	+0.082
	−	+	+0.084	+0.048	+0.002
	−	−	−0.151	−0.082	0.000
	Total		−1.245	−1.246	−1.205
Total	+	+	−10.222	−10.262	−9.803
	+	−	+1.002	+0.662	+0.251
	−	+	+0.387	+0.213	+0.007
	−	−	−1.171	−0.623	−0.001
	Total		−10.005	−10.008	−9.546

[a]The NP correction in the Feynman gauge.
[b]The NP correction in the Coulomb gauge.
[c]The NP correction in the Coulomb gauge without transverse part.

namely, with only the positive-energy states of ^{16}O, the NP correction for the $1s_{1/2}$ in Table III is −10.101 eV in the Feynman gauge, while −10.492 eV in the Coulomb gauge hence the gauge dependence is 0.391 eV. On the other hand, after the inclusion of the antinucleon states, it is −10.910 eV in the Feynman gauge and −10.913 eV in the Coulomb gauge hence the gauge dependence is reduced to only 0.003 eV. We can see the similar effect of antinucleon states in Table IV, too. This shows that the antinucleon states have an important role for the gauge invariance of the two-photon exchange process involving the nucleus even in this light muonic atoms where the relativistic effects are not so large.

Why the antinucleon states provide a non-negligible effect on the NP correction can be understood as follows. The transverse form factors which connect upper and lower components of Dirac spinors become large in the transition to the negative-energy states due to the inversion between the large and small components of Dirac spinors. Since the form factor to the highly excited states usually has a peak around the momentum corresponding excitation energy, it may be expected that the form factor of antinucleon states with the excitation energy more than 1 GeV cannot overlap with those of the muon, in which the excitation energies are taken into account up to ±250 MeV in the present calculation. For the antinucleon states which are bound strongly, however, this is not the case and the peak of a form factor appears in the considerably low momentum region as shown in Fig. 2(a). Consequently, large transverse form factors in antinucleon states can overlap enough with form factors of muon and contribute to the NP correction visibly. Comparing the contributions in the fourth and fifth columns and the Coulomb NP contributions in the last columns in Tables III and IV, one can confirm that almost all of the antinucleon contribution comes from the transverse contributions.

In the NP calculation with the nonrelativistic RPA, there exists a large violation of gauge invariance, when only the ladder and cross diagrams are taken into account. It was then found that the seagull diagram was necessary for the gauge invariance [3,4]. Therefore, it is interesting to see whether the effect of antinucleon states corresponds to the effect of the seagull diagram in the nonrelativistic nuclear model in the NP correction (see Fig. 4). Indeed, these two effects are analogous to each other; namely, the contribution from the antinucleon states to the NP correction mostly comes from the transverse-photon exchange, while the seagull diagram involves only the transverse-photon field.

For quantitative comparison, we have calculated the muonic NP correction for ^{16}O in the collective model [21,28], in which the excitation modes are assumed to be concentrated in a single resonant state for each spin λ and isospin τ with excitation energies given by

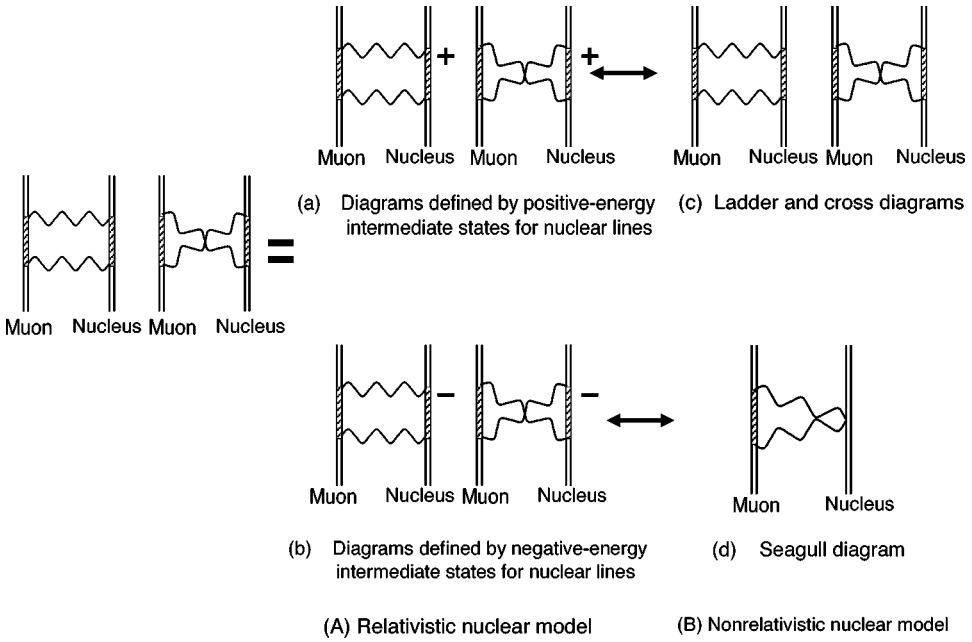

FIG. 4. The relation between the relativistic and nonrelativistic nuclear models in the two-photon exchange diagrams. The contribution from the antinucleon states in the relativistic nuclear model corresponds to the seagull diagram in the nonrelativistic nuclear model if the positive-energy excitations calculated by the relativistic nuclear model agree with the excitations calculated by the nonrelativistic nuclear model.

$$\omega_N = \begin{cases} [100(1-\tau)+200\tau](1-A^{-1/3})A^{-1/3} & \text{for } \lambda = 0, \\ 95(1-A^{-1/3})A^{-1/3} & \text{for } \lambda = 1, \\ [75(1-\tau)+160\tau](1-A^{-1/3})A^{-1/3} & \text{for } \lambda \geqslant 2. \end{cases} \tag{23}$$

In Table V, we show the results with the effective mass generated from MFT and with the ordinary nucleon mass (numbers in parenthesis). The comparison reveals that for the net NP correction, the results with the effective mass reproduces the relativistic results better as in the case of the EWSR. It may be expected that the EWSR value gives a good prediction for the NP estimate of the light muonic atoms as well as the electronic atoms. The contribution to the NP energy from 1^- state, however, is smaller than that of the RRPA in spite of the result that the EWSR value of nonrelativistic model with effective mass is enhanced over that of the relativistic calculation. This discrepancy may be attributed to the difference between the nuclear excitation energies given by Eq. (23) and the RRPA calculation. In particular, the NP effects with the collective model are more sensitive to the excitation energy since the excitations have only one collective state for each spin-parity mode.

For the contribution of the seagull diagram, on the other hand, only the charge distribution of the nuclear ground state is required together with the nucleon mass. Therefore, the seagull diagram is mostly independent of the model. The total contributions of seagull diagram with the effective mass are −0.898 eV and −0.473 eV in the Feynman and Coulomb gauges, respectively. Comparing with Table III, in which the contributions of antinucleon states are −0.808 eV in the Feynman gauge, while −0.421 eV in the Coulomb gauge, it is confirmed numerically that the correction due to the seagull diagram with the effective mass agrees with the contribution from the antinucleon states very well.

We have shown that the antinucleon states have an important role in the nuclear-polarization calculation. As discussed above, however, it should not be concluded that the nonrelativistic treatment of nucleus cannot provide reliable estimate of the NP correction since the contribution of the antinucleon states is similar to that of seagull diagram which arises from the nonrelativistic treatment of the nucleus. Hence, as far as the present numerical estimate of the NP energy shifts is concerned, there exists an essential equivalence between the nonrelativistic treatment of NP and the relativistic calculation with RRPA based on QHD in which the energy dependence in Eq. (15) is ignored. As seen in Table V, on the other hand, we have to note that present relativistic results are somewhat enhanced over nonrelativistic one if the usual nucleon mass is used in the nonrelativistic calculation. The effective mass effect in the NP correction may give the explanation of the anomaly in the Δp fine-structure splitting energies of muonic heavy atoms, in which the nuclear polarization contributes to the muonic levels at a keV [4,29].

It is extremely important to carry out a similar analysis for electronic NP correction in heavy atoms, where it is expected that the effect of antinucleon states is more remarkable in order to obtain the gauge-invariant result [3,28]. The investigation of the antinucleon contribution to the NP corrections in electronic ground and excited states as well as muonic states may provide an evidence of the strong attractive self-energy of antinucleon in the nucleus.

IV. SUMMARY

We have evaluated the NP correction to the $1s_{1/2}$ state of muonic ^{16}O using the RRPA on the MFT basis and obtained the similar results between the linear and the nonlinear nuclear models. By relativistic treatment, the antinucleon states, as well as the antimuon states, both of which represent the blocking effect of the response of vacuum, appear in the intermediate states and contribute to the NP correction. The transverse form factor of the bound antinucleon state has a

TABLE V. Same as Table III except for the nonrelativistic (collective) model is employed in the NP calculation. The seagull diagram contributes to the NP correction (denoted by SG in second column) instead of the contribution from antinucleon states. The effective mass from the MFT calculation with HS is taken into account in the NP calculation. In the parenthesis, the result with ordinary mass of nucleon is also shown for comparison.

λ^π	ω_N	ω_μ	Feynman[a]	Coulomb[b]	CNP[c]
0^+	+	+	−0.894(−0.680)	−0.896(−0.682)	−0.896(−0.682)
	+	−	+0.068(+0.052)	+0.057(+0.043)	+0.057(+0.043)
	SG	+	+0.019(+0.014)	+0.000(+0.000)	
	SG	−	−0.036(−0.027)	−0.000(−0.000)	
	Total		−0.843(−0.641)	−0.839(−0.639)	−0.839(−0.639)
1^-	+	+	−6.968(−4.792)	−6.992(−4.809)	−6.673(−4.589)
	+	−	+0.849(+0.584)	+0.518(+0.356)	+0.138(+0.095)
	SG	+	+0.315(+0.203)	+0.179(+0.114)	
	SG	−	−1.114(−0.738)	−0.609(−0.401)	
	Total		−6.918(−4.743)	−6.904(−4.740)	−6.535(−4.494)
2^+	+	+	−2.177(−1.657)	−2.188(−1.665)	−2.148(−1.635)
	+	−	+0.196(+0.149)	+0.176(+0.134)	+0.145(+0.110)
	SG	+	+0.101(+0.075)	+0.057(+0.042)	
	SG	−	−0.183(−0.140)	−0.100(−0.076)	
	Total		−2.063(−1.573)	−2.055(−1.565)	−2.003(−1.525)
Total	+	+	−10.039(−7.129)	−10.076(−7.156)	−9.717(−6.906)
	+	−	+1.113(+0.785)	+0.751(+0.533)	+0.340(+0.248)
	SG	+	+0.435(+0.292)	+0.236(+0.156)	
	SG	−	−1.333(−0.905)	−0.709(−0.477)	
	Total		−9.824(−6.957)	−9.798(−6.944)	−9.377(−6.657)

[a]The NP correction in the Feynman gauge.
[b]The NP correction in the Coulomb gauge.
[c]The NP correction in the Coulomb gauge without transverse part.

large overlap with that of muon. Therefore, the contribution of antinucleon states is non-negligible in the NP correction though the energy denominators are considerably large. Even in the NP correction for the light muonic atom as ^{16}O, there is a 4–8% effect of antinucleon states and it is essential for gauge invariance.

For muonic ^{16}O, we could obtain the result that the correction due to the seagull diagram and the contribution from the antinucleon states agree fairly well. Consequently, the relativistic QHD gives similar results with the nonrelativistic results by taking into account the effective mass. However, it remains to be studied for heavy muonic and electronic atoms, for which the NP effects can be measured experimentally. The NP effects in these atoms may depend rather sensitively on the details of the relativistic nuclear models. The quantitative estimate of NP effects with the QHD-type models may provide information on the strong binding of the antinucleon.

ACKNOWLEDGMENTS

This work was supported by Matsuo Foundation, Suginami, Tokyo. A.H. would like to thank Professor S. Kita for giving him the opportunity to do this work and discussion.

APPENDIX: GAUGE INVARIANCE IN THE NUCLEAR POLARIZATION

In the nuclear-polarization tensor defined by

$$\Pi_N^{\xi\zeta}(\omega,\boldsymbol{q},\boldsymbol{q}') = \sum_{I'} \left(\frac{J_N^{\xi}(\boldsymbol{q})_{II'} J_N^{\zeta}(-\boldsymbol{q}')_{I'I}}{\omega - \omega_N + iE_{I'}\epsilon} - \frac{J_N^{\zeta}(-\boldsymbol{q}')_{II'} J_N^{\xi}(q)_{I'I}}{\omega + \omega_N - iE_{I'}\epsilon} \right), \tag{A1}$$

we assume the completeness of the nuclear intermediate states and the charge-current conservation in the transition densities. Then, multiplying Eq. (A1) by q_μ, one obtains

$$\begin{aligned} q_\mu \Pi_N^{\mu\nu}(\omega,\boldsymbol{q},\boldsymbol{q}') = \sum_{I'} & (\langle I|\hat{\varrho}_N(-\boldsymbol{q})|I'\rangle\langle I'|\hat{j}_N^{\nu}(\boldsymbol{q}')|i\rangle \\ & - \langle I|\hat{j}_N^{\nu}(\boldsymbol{q}')|I'\rangle\langle I'|\hat{\varrho}_N(-\boldsymbol{q})|I\rangle) \\ & = \langle I|[\hat{\varrho}_N(-\boldsymbol{q}),\hat{j}_N^{\nu}(\boldsymbol{q}')]|I\rangle. \end{aligned} \tag{A2}$$

It is well known that Eq. (A2) must vanish if the gauge invariance is satisfied in the sum of the ladder and cross

diagrams. For the electromagnetic charge and current operators of the nucleus,

$$\hat{\varrho}_N(-\boldsymbol{q}) = \sum_i^A \mathcal{Q}\begin{pmatrix} 1 & 0 \\ 0 & 1 \end{pmatrix} e^{i\boldsymbol{q}\cdot\boldsymbol{r}_i},$$

$$\hat{j}_N(\boldsymbol{q}') = \sum_i^A \left[\mathcal{Q}\begin{pmatrix} 0 & \boldsymbol{\sigma} \\ \boldsymbol{\sigma} & 0 \end{pmatrix} e^{-i\boldsymbol{q}'\cdot\boldsymbol{r}_i} + \frac{\kappa_N}{2M}\boldsymbol{\nabla}_i \cdot \begin{pmatrix} \boldsymbol{\sigma} & 0 \\ 0 & -\boldsymbol{\sigma} \end{pmatrix} e^{-i\boldsymbol{q}'\cdot\boldsymbol{r}_i} \right], \tag{A3}$$

used in the present paper, the commutation relation in Eq. (A2) vanishes and hence, the relation leading to the gauge invariance $q_\mu \Pi_N^{\mu\nu}(\omega, \boldsymbol{q}, \boldsymbol{q}') = 0$ follows.

The charge-current operators indicated in Eqs. (16) and (17), on the other hand, do not commute due to the second term of the right-hand side in Eq. (16). Therefore this contribution results in gauge dependence when the ladder and cross diagrams only are considered. The gauge invariance with the charge-current operators of Eqs. (16) and (17) is achieved if the seagull contribution is also included. To see this, consider the reduction formula for the polarization propagator of virtual photon [30]:

$$(2\pi)^4 \delta(k' + P_\beta - k - P_\alpha)\Pi^{\mu\nu} = -i \int d^4x d^4y e^{-ik'x} e^{-iky} \Big\{ \langle\beta|T[J^\mu(x)J^\nu(y)]|\alpha\rangle - \delta(x^0 - y^0)\langle\beta|[J^\mu(x), \dot{A}^\nu(y)]|\alpha\rangle$$
$$- \frac{\partial}{\partial y^0}[\delta(x^0 - y^0)\langle\beta|[J^\mu(x), A^\nu(y)]|\alpha\rangle] \Big\}. \tag{A4}$$

The last term of the right-hand side usually vanishes. In fact, adding the gauge fixing term and using the indefinite metric quantization of the electromagnetic field, the canonical electromagnetic field A_μ commutes with the electromagnetic current of Eqs. (16) and (17) too. The second term of the right-hand side is the so-called seagull contribution

$$\Pi_{SG}^{\mu\nu} = [\dot{A}^\mu(x), J^\nu(y)]_{x^0=y^0}. \tag{A5}$$

Writing $\dot{A}^\mu(x)$ in terms of the canonical variables it is possible to show that $\Pi_{SG}^{0\nu}$ vanishes and

$$[\dot{A}^i(x), J^\nu(y)]_{x^0=y^0} = -\frac{\kappa_N}{2M_N}[\hat{\bar{\psi}}(x)\sigma^{0i}\hat{\psi}(x), J^\nu(y)]_{x^0=y^0}. \tag{A6}$$

It can be easily seen that the four-divergence of this seagull term cancels the nonvanishing term of the $[\varrho(x), J^\nu(y)]$ showing the gauge invariances of the model.

[1] E. Borie and G. A. Rinker, Rev. Mod. Phys. **54**, 67 (1982).
[2] P. J. Mohr, G. Plunien, and G. Soff, Phys. Rep. **293**, 227 (1998).
[3] A. Haga, Y. Horikawa, and Y. Tanaka, Phys. Rev. A **65**, 052509 (2002).
[4] A. Haga, Y. Horikawa, and Y. Tanaka, Phys. Rev. A **66**, 034501 (2002).
[5] Y. Horikawa and A. Haga, Phys. Rev. C **67**, 048501 (2003).
[6] J. L. Friar and M. Rosen, Ann. Phys. (N.Y.) **87**, 289 (1974).
[7] R. Rosenfelder, Nucl. Phys. **A393**, 301 (1983).
[8] B. D. Serot and J. D. Walecka, Adv. Nucl. Phys. **16**, 1 (1986).
[9] R. J. Furnstahl, Phys. Lett. **152B**, 313 (1985).
[10] P. G. Blunden and P. McCorquodale, Phys. Rev. C **38**, 1861 (1988).
[11] M. L'Huillier and N. Van Giai, Phys. Rev. C **39**, 2022 (1989).
[12] C. J. Horowitz and J. Piekarewicz, Nucl. Phys. **A511**, 461 (1990).
[13] Z. Ma, N. Van Giai, H. Toki, and M. L'Huillier, Phys. Rev. C **55**, 2385 (1997).
[14] Z. Y. Ma, H. Toki, and N. Van Giai, Nucl. Phys. **A627**, 1 (1997).
[15] J. R. Shepard, E. Rost, and J. A. McNeil, Phys. Rev. C **40**, 2320 (1989).
[16] J. F. Dawson and R. J. Furnstahl, Phys. Rev. C **42**, 2009 (1990).
[17] P. Ring, Z. Y. Ma, N. Van Giai, and D. Vretenar, Nucl. Phys. **A694**, 249 (2001).
[18] J. Piekarewicz, Phys. Rev. C **64**, 024307 (2001).
[19] M. Gell-Mann and F. Low, Phys. Rev. **84**, 350 (1951).
[20] J. Sucher, Phys. Rev. **107**, 1448 (1957).
[21] G. Plunien, B. Müller, W. Greiner, and G. Soff, Phys. Rev. A **39**, 5428 (1989); Phys. Rev. A **43**, 5853 (1991).
[22] C. J. Horowitz and B. D. Serot, Nucl. Phys. **A368**, 503 (1981).
[23] Y. K. Gambhir, P. Ring, and A. Thimet, Ann. Phys. (N.Y.) **198**, 132 (1990).
[24] G. A. Lalazissis, J. König, and P. Ring, Phys. Rev. C **55**, 540 (1997).
[25] Y. Sugahara and H. Toki, Nucl. Phys. **A579**, 557 (1994).
[26] N. Ullah and D. J. Rowe, Nucl. Phys. **A163**, 257 (1971).

[27] A. Bohr and B. R. Mottelson, *Nuclear Structure* (Benjamin, New York, 1975), Vol. 2, p. 399.
[28] N. Yamanaka, A. Haga, Y. Horikawa, and A. Ichimura, Phys. Rev. A **63**, 062502 (2001).
[29] P. Bergem, G. Piller, A. Rueetschi, L. A. Schaller, L. Schellenberg, and H. Schneuwly, Phys. Rev. C **37**, 2821 (1988).
[30] S. L. Adler and R. F. Dashen, *Current Algebras and Applications to Particle Physics* (Benjamin, New York, 1968), p. 218.